Direction Selectivity in the Middle Lateral and Lateral (ML and L) Visual Areas in the California Ground Squirrel

Monica Paolini and Martin I. Sereno

Cognitive Science, University of California, San Diego, La Jolla CA 92093-0515, USA

Extracellular recordings obtained from the extrastriate cortex of the California ground squirrel, a diurnal sciurid, show that large receptive fields and a strong direction selectivity are present in the middle lateral area (ML) and the lateral area (L), located laterally to V2 and V3. Direction selectivity was tested by presenting stimuli of varying dimensions, shapes and speeds at different locations in the visual field. Most cells in ML and L (84%) were direction selective, with a preference for fast speeds, indicating that these areas share a role in motion processing. Areas ML and L may be homologous to area MT or may represent a case of homoplasia. A directional anisotropy for motion towards the vertical meridian was found in ML and L cells, suggesting that these areas may be involved in detecting predators and other moving objects coming from the periphery, rather than in processing flow fields caused by forward locomotion, for which a centrifugal bias might be expected.

Motion processing has been widely studied in primates and cats. There is large agreement that, beyond V1, some extrastriate areas are specialized for motion processing and, in primates at least, are preferentially driven by the magnocellular LGN pathway (DeYoe and Van Essen, 1988; Livingstone and Hubel, 1988; Andersen *et al.*, 1990; Maunsell *et al.*, 1990; Wurtz *et al.*, 1990; Van Essen *et al.*, 1992; Young, 1992). In primates area MT appears to be selective for translational object motion, especially when the motion of the object contrasts with that of the background (Baker *et al.*, 1981; Maunsell and Van Essen, 1983; Albright, 1984; Felleman and Kaas, 1984; Allman *et al.*, 1985). In cats the lateral suprasylvian areas, including PMLS, have been shown to be specialized for motion processing (Spear and Baumann, 1975; von Grunau and Frost, 1983; Blakemore and Zumbroich, 1987; Gizzi *et al.*, 1990; Payne, 1993; Toyama *et al.*, 1994; Wang *et al.*, 1995).

The presence of an area homologous to MT in other species has been widely discussed but there is no consensus on how widely distributed an MT-like area is among mammals. The lateral suprasylvian areas (LS) in the cat have often been considered to be homologous to MT (Payne, 1993), although the homology has recently been questioned (Kaas, 1995; Northcutt and Kaas, 1995). Among rodents there is great variation in the organization of visual cortical areas, especially between diurnal species, who rely more on visual information, and nocturnal species, who rely more on non-visual sensory input. Whether any specialization for motion processing is present in specific regions in rodent extrastriate cortex is currently unclear. This study attempts to address that question.

In the rat, a nocturnal animal with a well-developed somatosensory system but poor vision, extrastriate cortical areas occupy less total area than area V1. The rat visual system also differs from that of primates in lacking color selectivity (Neitz and Jacobs, 1986) and an obvious magno–parvo and dorsal–ventral pathway distinctions (Montero *et al.*, 1973; Olavarria and Montero, 1984; Coogan and Burkhalter, 1993; Lund *et al.*, 1993; Montero, 1993).

Squirrels, by contrast, are diurnal rodents with a highly sophisticated visual system in which striate and extrastriate cortex occupies a much larger portion of the cortex. The squirrel-to-rat ratio for the area of striate cortex is 4:1. For extrastriate cortex, it is a striking 8:1. By contrast, the squirrel whisker barrel field is small – only one-third the size of that in the rat (in absolute area).

A detailed map of retinotopic organization in striate and extrastriate cortex has been established for squirrels (Hall *et al.*, 1971; Kaas *et al.*, 1972; Cusick *et al.*, 1980; Montero and Cliffer, 1981; Gould, 1984; Revishchin and Polkoshnikov, 1987; Kaas *et al.*, 1989; Sereno *et al.*, 1991). Area V1 in squirrels has three distinct compartments, clearly visible in the myelin stain of a flat-mounted cortex (Fig. 1): a medial monocular region, a binocular region, along the lateral border of the monocular region, and a bilateral binocular region (one location in one retina drives neurons in both the contralateral as well as the ipsilateral hemisphere), between the binocular region and V2 (Kaas *et al.*, 1972, 1989; Gould, 1984; Sereno *et al.*, 1991). A continuous V2 is located along the rostral border of V1, in contrast with other nocturnal rodents, like the rat, in which several areas, each with its own retinotopic representation, directly adjoin the V1 border. The areas studied here are located lateral to V2. Areas L and ML (lateral and middle lateral) have a light myelination pattern and larger receptive fields than areas V1 and V2. Findings from mapping (Sereno *et al.*, 1991) and connection studies (Kaas *et al.*, 1989) led us to speculate that areas ML and L might be stations in a pathway devoted mainly to motion processing, perhaps similar to the dorsal magnocellular pathway in primates. The cortical region occupied by areas ML and L is approximately coextensive with connectionally defined areas OT_r and OT_c (Kaas *et al.*, 1989), and appears to receive direct V1 input (Kaas *et al.*, 1989).

There are practical advantages to choosing squirrels as a visual system model. Squirrels have excellent eye optics (Gur and Sivak, 1979; McCourt and Jacobs, 1984b) and a cortex without sulci that can be easily flattened, and they are very robust experimental subjects. For these reasons, they provide a viable alternative to primates, especially in experiments requiring a large number of animals.

Direction selectivity was tested in areas ML and L in the California ground squirrel, *Spermophilus beecheyi*, using stimuli of different sizes and shapes, moving in different directions and at different speeds. Stimulus sets were presented either in the center of the receptive field or at up to 36 locations, to test for local direction selectivity to translational motion. Some of the data have been previously presented in abstract form (Paolini *et al.*, 1995).

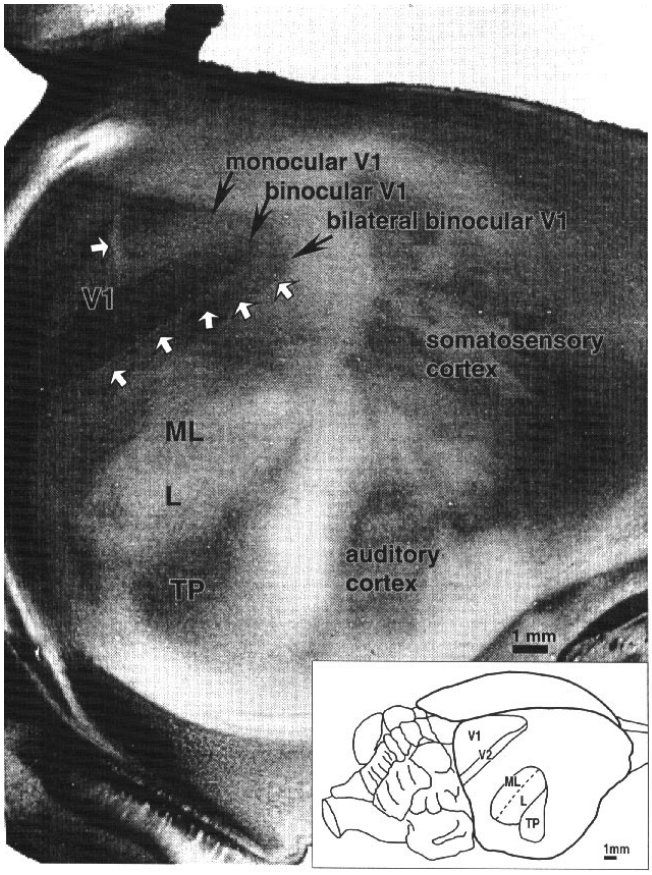

Figure 1. Myelin stain of flat-mounted squirrel cortex. Area V1 is characterized by heavy myelination in all of its three subdivisions: monocular, binocular and bilateral binocular. The border between V1 and V2 is indicated by multiple white arrows. The representation of the optic nerve head (*blind streak*) is also visible in the central part of V1 (indicated by a single white arrow) as a lightly myelinated area. Far lateral to V1 is the teardrop-shaped area TP, recognizable by its darker staining. Areas ML and L lie between areas V1, V2 and TP laterally, and have a lighter myelination than surrounding areas. Most of the cortex is visible, including auditory and somatosensory cortex. Top-left corner: posterior; bottom-right corner: lateral. Right bottom corner: drawing of a squirrel brain (anterior to the right), showing the relative position of the areas shown in the flat-mount.

Materials and Methods

Animal Preparation

Fifteen adult male and female California ground squirrels (*S. beecheyi*) were trapped from their natural habitat in Southern California. Their weight ranged from 350 to 800 g. The animals were kept for a limited time in an animal care facility.

Squirrels were initially anesthetized with ketamine (Ketaset, 150 mg/kg i.p.) followed by an injection of urethane (0.5 g/kg i.p.), and were kept anesthetized by subsequent smaller injections of urethane (0.08 g/kg) at intervals of 8–24 h as needed. During the surgery, lidocaine (Xylocaine 2.5%) was used as a topical anesthetic. Ringer's solution was injected subcutaneously every few hours to prevent dehydration.

In preparation for recording, the animal was placed in a stereotaxic instrument and an aluminum post was attached to the frontal part of the skull with screws and dental cement to keep the head of the animal fixed without pressure points during the electrode penetrations. A craniotomy was made in the right hemisphere over the portion of visual cortex of interest and the dura was removed to visualize cortical blood vessels, and to avoid damage to the cortex and to the electrode. The exposed brain was covered with viscous sterile silicone oil to prevent dehydration of the cortical surface and to reduce pulsation.

The cornea was anesthetized with a long-lasting topical anesthetic (0.7% dibucaine HCl) dissolved in contact lens wetting solution. Pupillary dilation was obtained by using Cyclogil 1%. The left eye was immobilized by cementing a thin eye ring to the margins of the cornea with cyanoacrylate tissue cement. The cornea was protected from drying by a film of light silicone oil. The eye of the California ground squirrel is emmetropic, i.e. with a refractive state close to zero (McCourt and Jacobs, 1984b). Corrective lenses were not necessary to satisfactorily bring the visual display into focus on the retina. Retinal focus was assessed with an ophthalmoscope. Squirrels have an extremely elongated optic nerve head in the retina that can be mapped and used to precisely check the eye position. This 'blind streak' is especially well suited to monitoring eye position because it provides a measure of eye rotation, as well as eye translation. The elongated optic nerve head and 4–5 identifiable blood vessels coming from it were mapped onto a translucent hemisphere by back-projecting their images with an ophthalmoscope. These retinal landmarks were repeatedly checked to ensure that the eye did not move during the recording session.

At the end of the experiment the squirrel was killed with an overdose of pentobarbital sodium (Nembutal). The brain was immediately removed and fixed (see Histological Analysis below). Surgical and experimental procedures received approval from the UCSD Office of Animal Resources. Wild animal trapping conformed with California Fish and Game regulations.

Recording Sessions

Tungsten electrodes [250 µm diameter, ~10 MΩ impedance, FHC (25-10-1733A), Brunswick, ME] were used to record extracellular electrophysiological activity. Stimuli were presented monocularly to the left eye and the cell activity was recorded from the right hemisphere. The electrodes were introduced into V1, V2 or V3 in the coronal plane but with the tip angled laterally ~20–25° from vertical, so that the electrodes were almost tangential to the cortical laminae when they reached ML and L.

Receptive Field Mapping

Receptive field position and extent were first mapped by hand on a translucent plastic hemisphere placed in front of the squirrel's eye using moving spots of light projected on the hemisphere in a dimly lit room. The position of the optic nerve was mapped onto the translucent hemisphere and used to estimate the location of the horizontal meridian visual streak, located ~16° above the optic nerve head in the visual field (Hall *et al.*, 1971). The vertical meridian was defined as the point of horizontal reversal in the retinotopic map. This was located by hand mapping all the well-defined receptive fields of the cells encountered during the electrode penetrations. The centers of the receptive fields were digitized in polar coordinates, where the eccentricity, e, is the distance in degrees from the center of the receptive field to the center of the visual field (the intersection of the horizontal and vertical meridians) and the polar angle, θ, is the angle between the horizontal meridian and the line from the center of the receptive field to the center of the visual field.

Receptive fields were also mapped on the computer screen to quantitatively confirm their position and extent. A small stationary bright square was presented at one of 100 locations within the visual field. Each square was presented for 160–250 ms and covered 2–5° of visual field, depending on the distance of the screen. The entire display covered a square 20–50° on a side. The size of the receptive fields mapped on the computer screen matched the size of the hand-mapped ones.

Moving Stimuli

Stimuli were presented at a moderately fast rate, in most cases with no interstimulus interval. When the interstimulus interval was added, its duration was set to be equal to that of the stimulus presentation. Twenty randomized repetitions of each stimulus set were presented. Several stimulus configurations were presented to each cell, usually over a period of 2–4 h. In most cases, we varied both the location and direction of individual stimulus sweeps. Only one stimulus was presented at a time. The speed and retinal size of the stimulus varied somewhat because the distance of the display monitor from the eye was adjusted to take some

account of the receptive field size. Within each stimulus set, the stimulus speed (or speeds, for multiple speed stimuli) and the stimulus size was constant. For stimuli presented at multiple locations, the entire area of visual field covered by stimuli was a square of 20–50° per side. Speeds ranged from 50 to 80°/s for all stimulus sets except for the multiple speed stimuli. The specific values for cell responses shown in figures are given in the legends. We used the following stimulus configurations:

1. *Circles at 36 locations*: a small bright circle moving in one of eight directions was presented in one of 36 locations in the visual field, for a total of 288 conditions. The diameter of the circles ranged from 2.5 to 6.2°. Each sweep lasted 80–250 ms.
2. *Short bar at 36 locations*: a short bright bar moving in one of eight directions was presented at one of 36 locations for 160 ms, without interstimulus intervals. The bars subtended 5–8° of visual field.
3. *Long bar at 36 locations*: a bright bar moving in one of eight directions was presented at one of 36 locations for 160 ms, without interstimulus intervals. The length of these bars was about three times the length of short bars (15–25°).
4. *Single bar*: a long bright bar moved in eight directions, at a single central location, for 330 or 660 ms, depending on the receptive field size estimated by hand mapping. The size of the bar was the same as in the long bar at 36 locations.
5. *Multiple speed stimuli*: a small bright circle at one location moved in one of eight directions at one of four different speeds (speed 1: 6–10°/s; speed 2: 12.5–20°/s; speed 3: 25–40°/s; speed 4: 50–80°/s). Stimuli at all speeds were shown for 660 ms and had a diameter of 2.5–6.2°.

The displays were generated by an Amiga 2500 and presented on a 27-inch NTSC monitor at 60 Hz in a non-interlaced mode, using software developed in the laboratory. The Amiga was connected to a single unit data acquisition system from DataWave, based on a 33 MHz Gateway 486DX, through serial and parallel lines. The onset of the stimulus was indicated by a parallel port pulse from the Amiga. The alignment of this pulse with the actual top of the ~16 ms NTSC frame was verified with a phototransistor (jitter ~1 ms).

Data Acquisition

The time of occurrence of spikes and stimulus onset pulse were recorded during the experiment with a 0.1 ms resolution using DataWave software. Latency was computed for each cell and for each stimulus set. First, the spikes collected from the stimulus onset were assigned to 10 ms bins and the spike count, s_c, was smoothed using the function:

$$s_c = \frac{r_{c-1} + 2 \cdot r_c + r_{c+1}}{4}$$

where r_c is the raw count for bin c (Vogels and Orban, 1990). For a given stimulus, latency was defined for those conditions in which the smoothed response, s_c, over three consecutive bins was larger than the averaged response across all the conditions. The latency for a single trial was the middle point of the first bin. The latency for the entire stimulus set was defined as the average of the latencies of the trials for which a latency had been defined.

The reverse correlation technique (Jones and Palmer, 1987; Palmer *et al.*, 1991; McLean *et al.*, 1994) was employed to analyze cell responses (Fig. 2). A continuous train of spikes was collected (Fig. 2*B*). For each stimulus, a temporal window was defined, starting at the stimulus onset plus the estimated cell latency and ending at the stimulus offset plus cell latency (Fig. 2*C*). All the spikes generated within this window were assigned to the current stimulus. The use of reverse correlation and the presentation of continuous sequences of short stimuli made it possible to collect a much larger amount of data than would have been possible with traditional methods.

Data Analysis

Preferred Direction

The preferred direction was defined as the angle of the vector sum of the response in the eight tested directions (Batschelet, 1981; Fisher, 1993; Zar, 1996). A direction of 90° indicates upward motion; a direction of 0° indicates motion towards the vertical meridian, for receptive fields in the left hemifield. The preferred direction, p, and the mean vector length, r_u, are defined using the x and y components of the vector sum of the response in the directions tested:

$$p = \tan^{-1}(y/x) \qquad r_u = \sqrt{x^2 + y^2}$$

$$x = \left(\sum_{d=1}^{n} s_d \cos a_d \right) \Big/ n \qquad y = \left(\sum_{d=1}^{n} s_d \sin a_d \right) \Big/ n$$

where n is the number of tested directions and s is the number of spikes for direction d, with direction angle a_d. A correction to r_u is needed to avoid the bias for grouped data and depends on the width of the grouping interval, i, here 45°, expressed in radians; the corrected r is defined as:

$$r = \frac{i}{2 \cdot \sin \frac{i}{2}} \cdot r_u$$

The length of the mean vector, r, is a measure of the concentration of the response, i.e. the strength of the direction selectivity. The value of r ranges from 0 to 1, where 1 indicates that the cell is firing only in the preferred direction and 0 that the spike distribution is uniform.

Because the direction index (DI) has often been used, we provide here the DI values along with the r values in the captions for comparison. The DI is defined as:

$$\mathrm{DI} = \frac{R_{\text{preferred-direction}} - R_{\text{antipreferred-direction}}}{R_{\text{preferred-direction}}} \cdot 100$$

and ranges from 0 to 100, with 100 representing the highest degree of selectivity. We put less emphasis on the DI because it provides a less comprehensive measure of the selectivity of a cell — it only considers the response in the preferred and antipreferred directions. Since information about other directions is lost, the DI sometimes provides a biased estimate of the strength of the direction preference (Fig. 3).

The mean angular deviation s is similar to the standard deviation for linear data, but it only ranges from 0 to 81°:

$$s = \frac{180}{\pi} \sqrt{2 \cdot (1 - r)}$$

The 100(1 – α)% confidence interval (CI) for the preferred direction was calculated as:

$$\mathrm{CI} = \left(p - \sin^{-1}\left(Z_{½\alpha} \cdot \sigma\right)\right), \quad \left(p + \sin^{-1}\left(Z_{½\alpha} \cdot \sigma\right)\right)$$

where $Z_{½\alpha}$ is the one-tailed-critical value Z for the chosen significance level, α, and σ is defined as follows:

$$\sigma^2 = \delta / n \quad \delta = (1 - r_2)/2r^2$$

where δ is the dispersion, n is the sum of spikes for each direction and r_2 is the mean resultant length of the doubled angle:

$$x_2 = \left(\sum_{d=1}^{n} s_d \cos 2a_d \right) \Big/ n \qquad y_2 = \left(\sum_{d=1}^{n} s_d \sin 2a_d \right) \Big/ n \qquad r_2 = \sqrt{x_2^2 + y_2^2}$$

Direction Selectivity

We used the Rayleigh test to test for direction selectivity (Fig. 3). The Rayleigh test compares the tuning curve against the uniform distribution. It relies only on the vector sum r and the number of spikes, N. The probability P that the tuning curve is not uniform is given by:

$$P = \exp\left(-Nr^2\right)$$

We defined those cells with $P < 0.001$ as direction selective.

Histological Analysis

At the end of each recording session, the cortex was either physically flattened or sectioned in the coronal plane, parallel to the electrode tracks. The lack of sulci in the squirrel cortex makes it possible to flatten the cortex with little distortion. Immediately after the brain was removed, the cortex was separated from the mesencephalon, brainstem and cerebellum, and the white matter removed with dry Q-tips (Olavarria and Van Sluyters, 1985; Tootell and Silverman, 1985). A small cut was made in the posterior cingulate cortex and the rostral pole to facilitate the unfolding and to reduce distortion. The cortex was flattened between

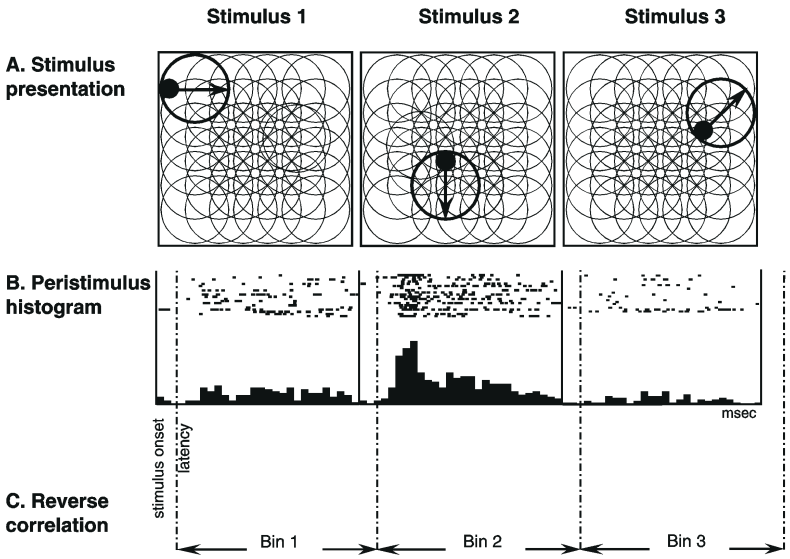

Figure 2. Stimulus presentation and data analysis. (*A*) A continuous sequence of three stimulus sweeps, uninterrupted by interstimulus intervals. Each stimulus consisted of a bright circle (represented in black in the figure). The circle was presented at 36 locations (thin circles), and moved in eight directions along the diameter of each circle, for a total of 288 conditions. The entire stimulus display covered a square portion of the visual field ranging from 30 to 50° per side. (*B*) Post-stimulus histograms and dot rasters of the cell activity. (*C*) Reverse correlation. After determining response latency, spikes in the time window starting at stimulus onset + latency and ending at the stimulus offset + latency were assigned to the current stimulus.

glass slides and fixed in 10% formalin with 20% sucrose added the next day. It was then attached to the stage of a freezing microtome at –15°C, cooled further and sectioned at 50 μm, and then stained for myelin the following day (Gallyas, 1979).

Electrode tracks were marked by lesions (15–20 μA for 10 s). In some cases, at the end of the recording session an elongated lesion was made by continuously applying current (15–20 μA) while retracting the electrode to help identify electrode tracks in flat-mounts.

Visual areas were identified by their myelination patterns. The V1 border is the most salient one. V1, V2 and TP are characterized by a heavy myelination pattern, while areas ML and L have lighter myelination. Because areas ML and L are contiguous and could not be easily distinguished from each other by the pattern of myelination, ML and L cells have for the time being been grouped together. A clear functional distinction between these two areas has not yet emerged.

In seven cases, the cortex was flattened and the reconstruction was limited to the portion of the electrode track crossing the gray matter. The identification of recording sites in the flat-mounted cortex allows particularly close correlation between recording sites and architectonic borders. In the other cases, the electrode tracks were reconstructed from coronal sections, which provide more information on laminar location but less precise correlation with subtle tangential myelin-defined borders than is possible with cortical flat-mounts.

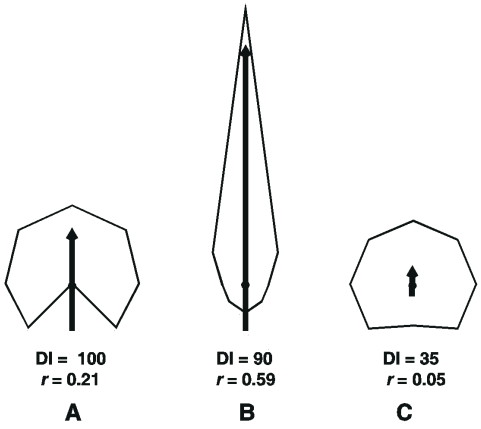

Figure 3. Response distributions quantified by direction index (DI) and vector sum (*r*). (*A*) Weak direction selectivity. The DI has a maximum value because there is no response in the anti-preferred direction despite the broad tuning. (*B*) Strong direction selectivity. The direction index is actually slightly lower; the vector sum, by contrast, gives a better estimate of the strength of direction selectivity. (*C*) No direction selectivity. Both the DI and *r* are very low in a case of uniform response.

Results

We recorded from 244 cells during 15 acute recording sessions. After the reconstruction of the electrode tracks, we determined that 192 cells were in areas ML and L. Those cells for which a latency could not be defined (i.e. they did not have a larger than average response in three consecutive bins) for any stimulus set were defined as visually non-responsive and were not further analyzed. The remaining 146 cells (76%) were considered visually responsive.

The extent and shape of the receptive field were mapped using a stationary square presented at 100 locations, arranged in a 10 × 10 grid. The stimuli were presented for 160 or 250 ms each, with no interstimulus interval, in 20 randomized repetitions of the complete sequence of 100 stimuli (Fig. 4). A sharp decline in the firing rate was used to determine the receptive field border. The average diameter of the receptive field cells we recorded from was 20.6° (n = 68, SD = 8.9) and the mean latency was 39 ms (n = 129). The average firing rate over the entire stimulus presentation was 10 spikes/s. The distribution of the receptive field locations is shown below in Figure 7.

Direction Selectivity in Areas ML and L

Among the 146 cells tested for direction selectivity in areas ML and L that were visually responsive to at least one set of stimuli, 122 (84%) were direction selective to at least one stimulus sequence. In most cases, direction selectivity was preserved across different stimulus types. Direction selectivity was determined using the Rayleigh test (P < 0.001). Unless otherwise noted, the response over the entire stimulus presentation (from

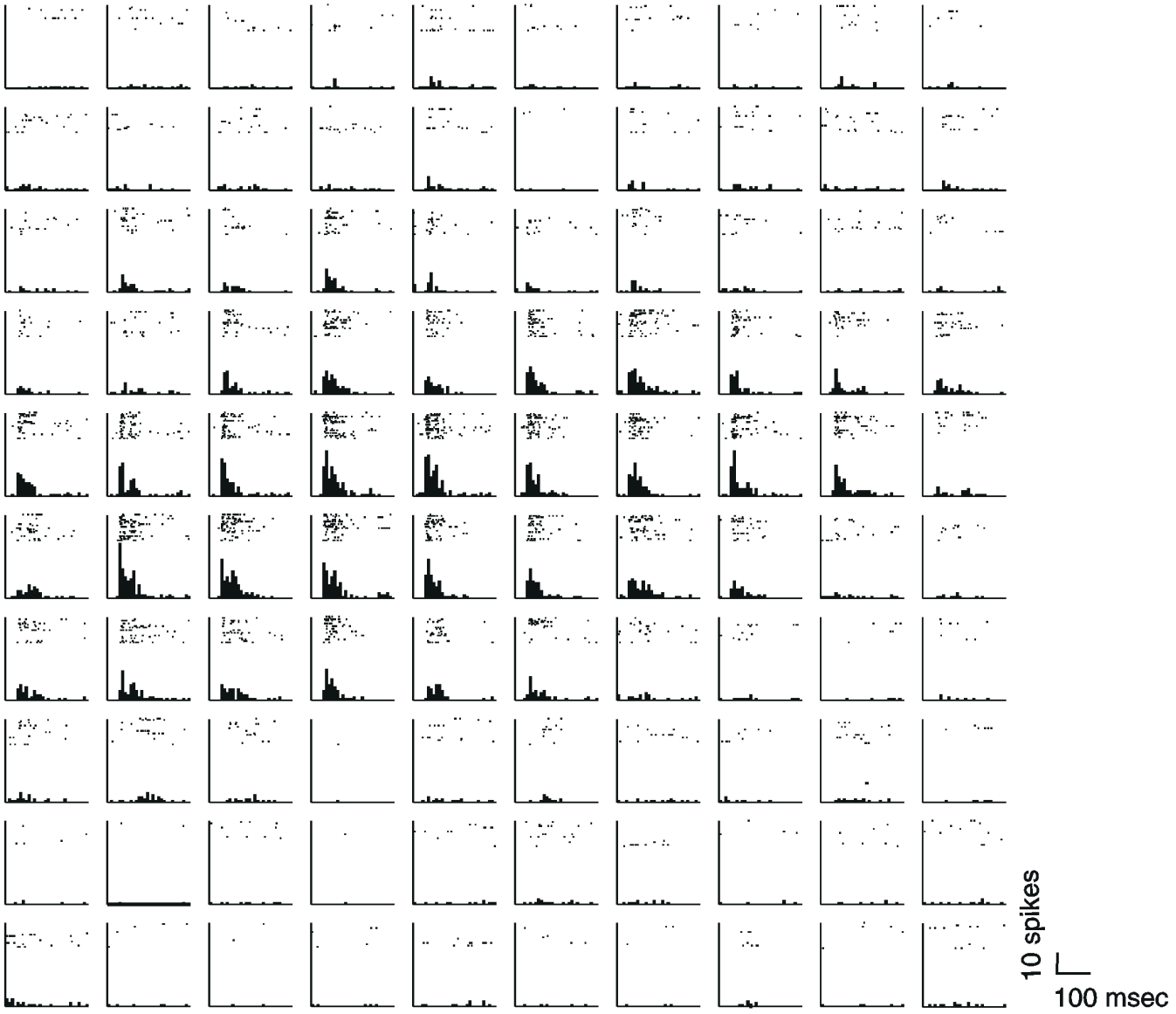

Figure 4. Quantitative receptive field plot for an ML/L neuron. The receptive field was mapped with small flashed squares presented one at a time at 100 locations on a 10 × 10 grid. Each histogram and dot raster represent the cell response at the corresponding stimulus location on the display monitor. The *x*-axis in the histograms and dot rasters begins at stimulus onset and ends at stimulus offset plus the estimated latency. In this case, histograms and dot rasters spanned 300 ms. Number of spikes per bin are shown on the *y*-axis. The response latency was 42 ms and the receptive field diameter was 25° ($e = 25$; $\theta = -18$). Each square side covered 2.5° of visual angle and there was a gap of 1° between squares. The entire grid occupied 34 × 34° of the visual field.

the stimulus onset + latency to stimulus offset + latency) was employed in the data analysis. For longer stimulus presentations, we also analyzed the response in the first 160 ms of the stimulus presentation to allow for a direct comparison of firing rate and direction selectivity strength across different stimulus sets.

Circles at 36 Locations

A small bright circle moving in one of eight directions for 80–250 ms was presented at 36 locations in the visual field, on a 6 × 6 grid (Fig. 2*A*), for a total of 288 stimulus conditions. The total area swept out by a stimulus depended on the duration of the presentation. A short interstimulus interval of the same duration as the stimulus sweep was sometimes added to the trials, but we could not discern a difference in the response between the two cases. The area covered by the eight different stimulus sweeps at each grid location partially overlapped in space with the area covered by stimuli at contiguous locations. Twenty shuffled sequences of the 288 stimuli were typically presented.

Among the 93 ML and L cells tested with this stimulus configuration, 74% (n = 69) were direction selective in at least six contiguous locations (Fig. 5). The r value averaged across locations and across cells was 0.36 (the average DI was 67); the average firing rate was 18 spikes/s. The average latency was 30 ms, 9 ms shorter than the latency for stationary stimuli. In almost all cases, the response was quite transient and dropped off well before the offset of the short stimulus sweep.

Short and Long Bars at 36 Locations

The effect of stimulus size was tested using bars of two sizes

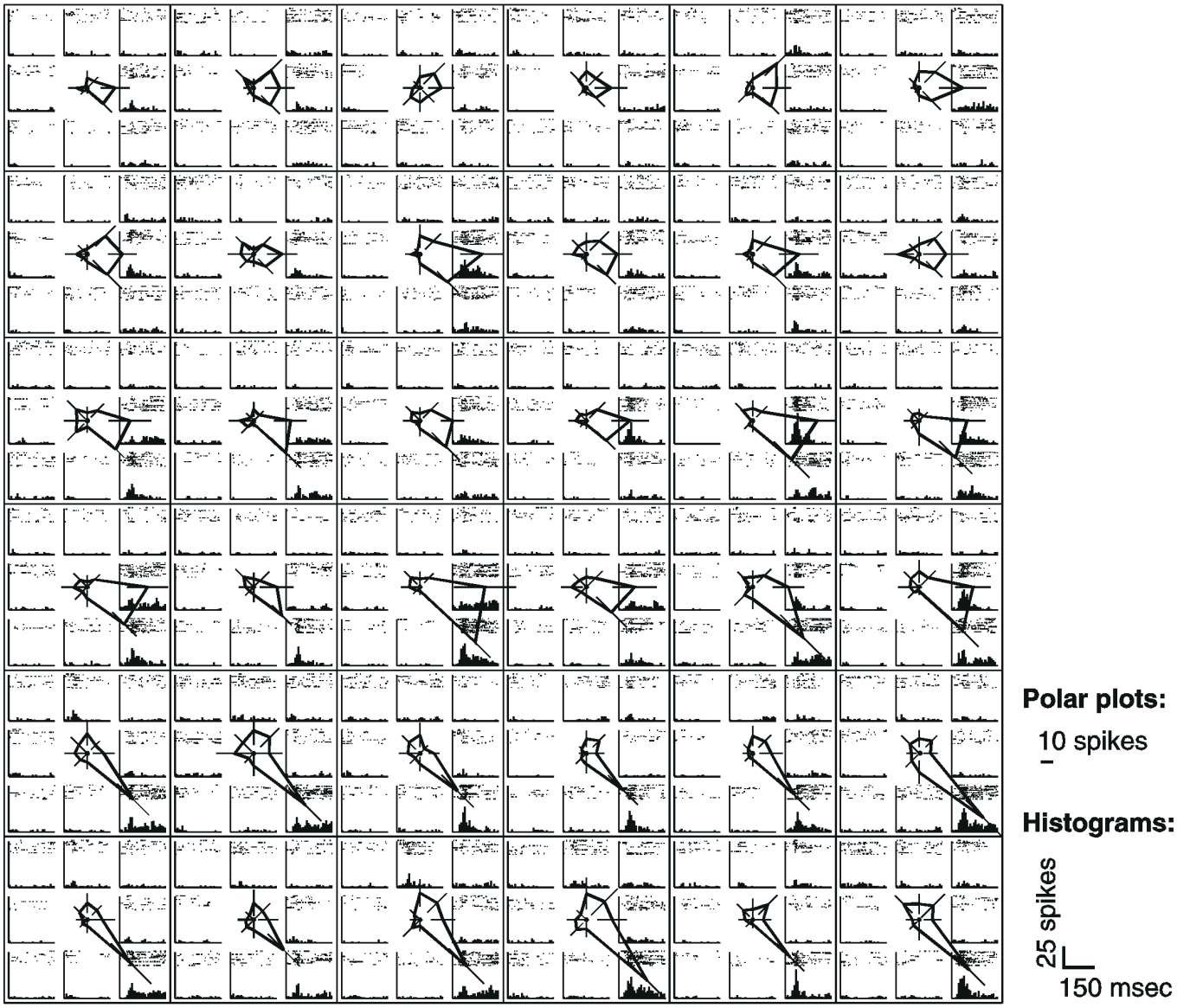

Figure 5. Response of an ML/L cell to a moving circle presented at 36 locations. The response of the cell was measured at 36 locations on a 6 × 6 grid. The eight histograms (10 ms bins) and dot rasters at each location show the response in the corresponding direction. The responses are also summarized by a polar plot in the center. Thin radial lines on the polar plots indicate the standard deviation of the response. Each stimulus circle subtended 4° of the visual field and moved at 29°/s, covering 11° of the visual field for each sweep. The area covered by the stimuli at all 36 locations was 31 × 31°. Each stimulus was presented for 250 ms with no interstimulus interval. Response latency was estimated to be 26 ms. The receptive field diameter was 10°, about one-third of the side of the entire display, and was located at the lower left where the firing rate was stronger and the direction-selective tuning sharper (e = 10; θ = –11). This cell is direction selective at all locations tested (r = 0.41, 99% CI = 9.9°, s = 62°, DI = 77; values averaged across locations), but a stronger direction-selective response was observed in the lower half of the stimulus display.

presented at 36 locations and moving in eight directions for 160 ms. The bar width was the same in both cases, but the long bar was slightly more than three times as long as the short bar (5–8° for the short bar, 16–25° for the longer bar). Among the cells tested with the long bar (n = 40), 63% were direction selective, with an average r of 0.30 (average DI = 57). Similarly, 65% of 46 cells were selective for shorter bars, with an average r of 0.32 (DI = 67). The latency was 40 ms for short bars and 46 ms for long bars; the firing rate was 10 spikes/s in both cases. Both stimulus sets were presented to 37 cells, of which 32 were direction selective. Among these, 18 cells (56%) were direction selective to both long and short bars, and the average difference among preferred directions was 13° (SD = 11.9); five cells were selective only to long bars and the other nine cells only to short bars. When compared with the response to the 6 × 6 circles stimuli, short and long bars show that preferred direction is preserved if stimulus size is changed. Except for stimulus shape and total area, circles and bars were defined by the same parameters, such as speed, number of locations and brightness. All cells tested (n = 9) with both circles and bars were selective to both stimulus sets. The average difference in preferred direction (averages across locations for each stimulus set) between circles and bars averaged across the 36 locations was only 14°.

Single Bar Stimulus

A uniformly bright bar centered in the middle of the display was moved in eight directions on a dark background. The length of the bar was 16–25° and the distance of the monitor was adjusted so that the bar length was scaled to approximate the receptive field diameter. The stimulus sweep was 330 or 660 ms, depending on the receptive field size, in most cases without an interstimulus interval. We tested 117 cells with the single bar stimulus and found 52 (44%) to be direction selective (Fig. 6). The average latency was 35 ms; the firing rate was 6 spikes/s and the average r was 0.18 (average DI = 42).

The size and speed of the stimulus were identical to the long bar stimuli presented at 36 locations and yet the percentage of direction-selective cells to the single bar was much lower (44 vs. 63%), as was the average value of r (0.18 vs. 0.30). One important difference between the stimulus sets is the length of the sweep duration: 160 ms for the bars at 36 locations and 330–660 ms for the single bar. The reduced firing rate in the single bar case (6 vs. 10 spikes/s) could have been due to the longer duration of the stimulus coupled with a similarly sharply transient response, or to interactions between successive sweeps. To test the hypothesis that stimulus duration had an effect on direction selectivity, we looked only at the first 160 ms of the response to the single bar stimuli, i.e. the duration of the stimulus presentation for short and long bars at 36 locations. The initial 160 ms portion of the response showed a remarkably stronger direction selectivity: 73% of the cells were direction selective (compared with the 42% for the entire stimulus presentation) and the average r was more than double (from 0.16 for the entire presentation to 0.34). The average DI also increased from 42 to 67. The firing rate was also higher (15 vs. 6 spikes/s), thus confirming that the response was transient in most cells.

The large increase in r for shorter stimuli suggests that the activity in the late part of the stimulus presentation was not simple noise (or a non-direction-selective response), because random (or uniform) addition to the spike count in all directions would have had a smaller effect on the r value. Instead, a structured response in the second part of the stimulus presentation is likely to be present and to be direction selective, but with a preferred direction different from that of the first part of the stimulus presentation [for similar temporal dynamics in orientation selective cells in V1 see Ringach *et al.* (1997)]. In fact, the peak during the second half of the response was often in the direction opposite to the preferred direction obtained in the first half of the stimulus presentation, as the stimulus left the receptive field (a small late response is visible in Fig. 6). Because no indication of such a change in the preferred direction was present when several locations in the visual field were tested with the same stimulus shape and speed, but for a shorter time, this secondary peak is suggestive of a spatio-temporal rather than exclusively spatial effect.

Multiple Speed Stimuli

A bright circle of 4–7° diameter, on a black background, centered in the middle of the display was moved in eight directions at four speeds (see Materials and Methods). All stimuli were presented for 660 ms; thus slow stimuli covered a smaller area than fast ones; however, all stimuli were centered on the receptive field. The average latency was 39 ms. Among the 13 cells tested 77% (n = 10) were direction selective and had a similar response pattern: at the two lowest speeds, the cell fired only rarely and direction selectivity emerged only at the two highest speeds, with the highest speed eliciting the strongest response. The firing rate at the two slowest speeds was respectively 4 (6–10°/s) and 5 spikes/s (12.5–20°/s), while at the two fastest speeds the firing rate was 7 (25–40°/s) and 9 spikes/s (50–80°/s). Among direction-selective cells, the r values for each speed, slowest to fastest, were: 0.16, 0.20, 0.25, 0.25; the averaged DI were: 42, 46, 54, 41.

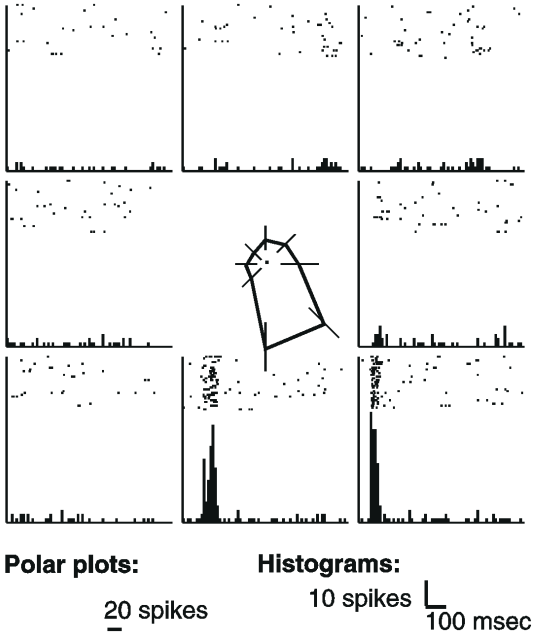

Figure 6. Response of an ML/L cell to a single bar moving in eight directions without any interstimulus interval. The preferred direction of the cell is 306° (r = 0.39, s = 63°, DI = 69), with a 99% confidence interval of 11°. The receptive field was located at the center of the display and the diameter was 21.5° (e = 23, θ = –45). The length of the bar was 16° and moved at a speed of 52°/s, covering a total of 35 × 35° of visual angle for each sweep. The latency was 54 ms.

When only the first 160 ms of the response interval were analyzed, a larger percentage (85 vs. 77%) of cells were direction selective and the overall direction selectivity was stronger (the average r was respectively 0.22, 0.27, 0.24, 0.48; the average DI was 47, 53, 72, 77). The firing rate also increased: for the two lowest speeds it was 14 and 15 spikes/s and for the two fastest speeds, 19 and 17 spikes/s.

Anisotropy

The distribution of the preferred directions was analyzed to determine if there was an overall preference for some direction. We found a preference for motion towards the vertical meridian in the 6 × 6 moving circles (n = 69; Rayleigh test, P < 0.01; r = 0.38; preferred direction = 17.66°) and the short and long bars presented at multiple locations (short bars: n = 40; P < 0.01; r = 0.72; preferred direction = 22.61°; long bars: n = 25; P < 0.01; r = 0.96; preferred direction = 3.71°).

In order to test for the presence of a centrifugal/centripetal pattern of preferred directions in the visual field, we computed the axial direction preference (Rauschecker *et al.*, 1987) by finding the angular difference between the preferred direction and the receptive field polar angle, θ (Blakemore and Zumbroich, 1987). A distribution of axial direction preferences with a peak at ~0° indicates a preference for centrifugal motion, while a peak at ~180° indicates a centripetal pattern. A peak at ~90 or –90° suggests a preference for, respectively, counterclockwise

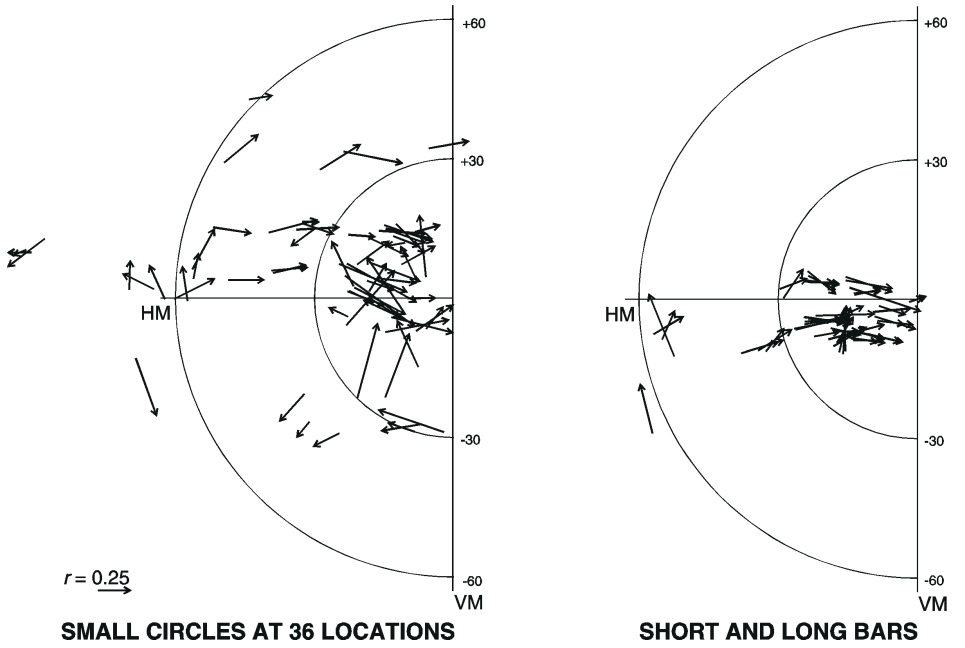

Figure 7. Distribution of receptive field locations and preferred directions. The location of receptive fields of cells tested with circles at 36 locations and with short and long bars at 36 locations is shown relative to the vertical meridian (VM) and the horizontal meridian (HM) in the left (contralateral) hemifield. Eccentricities of 30 and 60° are indicated by semicircles. The center of the receptive field is the middle point of the arrows. Preferred direction is indicated by the arrows direction, while the strength of direction selectivity (*r*) is indicated by the length of the arrow.

and clockwise rotation. The distribution of axial direction preferences points toward a preference for centripetal motion for both short ($P < 0.01$; $r = 0.68$; preferred direction = –168.81°) and long bars ($P < 0.01$; $r = 0.97$; preferred direction = –162.73°). In the case of the moving circles, a bias was clearly present ($P < 0.01$; $r = 0.43$), but the preferred direction (–134°) suggested a weaker centripetal preference coupled with a clockwise rotational bias.

Because there was an overabundance of several receptive fields near the horizontal meridian, where a preference for motion toward the vertical meridian is consistent with a preference for centripetal motion, the data cannot be used to decide between these two possible interpretations.

Discussion

Direction Selectivity in Areas ML and L

Direction selectivity was tested in areas ML and L, two lateral extrastriate areas of the ground squirrel cortex that receive direct V1 input and have rather large receptive fields. Most cells (84%) in areas ML and L are directionally selective, indicating that these areas may be part of a pathway specialized in motion processing, similar to the dorsal pathway in primates. More anatomical data about cortico-cortical patterns of connections and further data on the functional role of other extrastriate areas adjacent to areas ML and L are necessary to test this hypothesis. A region with a high density of direction-selective cells has never been reported before in extrastriate cortex in squirrels or other rodents. Because of the lack of data about other rodents, it is not known whether there are homologues of ML and L in rats. Areas LI and LL in rats (Montero, 1993) are in a similar location and do not directly adjoin the V1 border. However, in this respect, these areas are also similar to squirrel area TP. ML and L cells were also found to prefer moderately high speeds, at least in the 50–80°/s range. Higher speeds were not tested, and it is possible that the peak in the speed tuning curve is beyond 50–80°/s. In contrast, in primate MT and feline LS, the strongest response is often elicited by somewhat slower stimuli [32°/s in macaques (Maunsell and Van Essen, 1983), 10°/s in the owl monkey (Baker *et al*., 1981) and 30°/s in cats (Spear and Baumann, 1975)]. This difference in the preferred speed may be related to the higher retinal speeds experienced by squirrels, who locomote closer to the ground than cats and primates.

A strong preference for directions towards the vertical meridian was observed in L and ML cells. Because a large number of receptive fields were located in proximity to the horizontal meridian, the preference for caudal to nasal directions is also consistent with a centripetal anisotropy. Anisotropy for different directions has been found in several visual areas in primates and cats. It has often been expressed as a centrifugal anisotropy, presumably associated with the processing of expanding flow fields generated during forward locomotion (Blakemore and Zumbroich, 1987; Rauschecker *et al*., 1987; Albright, 1989; Bauer and Dow, 1989; Bauer *et al*., 1989). [For evidence against a widespread presence of anisotropy in areas involved in motion processing see Sherk *et al*. (1995).] Of course, eye and head movements add rotational and translational components to the expanding flow during locomotion, generating, at the retinal level, more complex flow fields than pure expansions (Gibson, 1950). Nevertheless, centrifugal direc- tions predominate during forward locomotion. The preference for *centripetal* motion, or motion *towards* the vertical meridian, suggests that areas ML and L may be more involved in detecting approaching predators and other moving objects on a collision course with the animal rather than in processing the flow field information generated during locomotion.

In both California ground squirrels (McCourt and Jacobs, 1984a) and gray squirrels (Blakeslee *et al*., 1985), a similar directional anisotropy for caudal to nasal directions in the visual field has been found in direction-selective ganglion cells in

the optic nerve. A preference for objects approaching the animal on a collision course was found in the pigeon's nucleus rotundus (Wang and Frost, 1992); however, these cells appear to compute the time-to-contact and only respond to motion in depth. In areas ML and L, by contrast, cells respond strongly to stimuli moving in a frontoparallel plane; also the transient response of ML and L neurons is quite different from the sustained response signaling time-to-contact in neurons in the nucleus rotundus.

Direction Selectivity Tests at Multiple Locations

We routinely tested for direction selectivity at several locations in the visual field. This increased the reliability of the data and, more importantly, allowed us to distinguish between genuine direction selectivity and simple response to stimulus onset. When testing direction selectivity at a single location, an artifactual direction-selective response can be elicited from a non-direction-selective cell responsive only to stimulus onset, if the stimulus onset locations for only a few contiguous directions are within the receptive field. By testing direction selectivity at different locations, with partially overlapping stimuli, we can reject such artifacts. If a homogeneous pattern of preferred directions emerges after testing at many different locations (Fig. 5), the response can be safely assumed to be truly direction selective. If the cell was responding to the onset of motion regardless of direction, a complex pattern of preferred directions would emerge – e.g. an expanding pattern visible only at the receptive field border.

Because of the large number of conditions that are required to test direction selectivity at multiple locations, it was necessary to limit the presentation time and to remove interstimulus intervals. However, the responses of most cells were sufficiently transient that the response to a given stimulus was limited to the first part of the stimulus sweep.

Evolution of Motion Processing in Mammals

The only cortical visual area unambiguously present in all mammals is V1, although the degree of laminar specialization varies widely. A continuous V2 adjoining the anterior or lateral border of V1 has also been found in several, but not all, mammals. Among rodents, for example, the rat (a myomorph rodent) and the degu (a caviomorph) (Olavarria and Mendez, 1979) lack a continuous V2.

Less is known about the evolution of most extrastriate areas. Area MT has been found in all primates and is characterized by a large concentration of direction-selective cells (Kaas, 1995; Krubitzer, 1995; Northcutt and Kaas, 1995). MT is a densely myelinated area that receives V1 input and is separated from the anterior border of V2 by at least one additional area (DL/V4). Area LS in the cat has often been proposed as an homologue of area MT (Zeki, 1974; Grant and Shipp, 1991; Payne, 1993). In the tree shrew, a lightly myelinated area, recipient of direct V1 input, along the anterolateral border of V2 has similar features to MT, suggesting that area MT may have developed from an area adjoined to the V2 border (Kaas, 1995; Krubitzer, 1995; Northcutt and Kaas, 1995).

Areas ML and L share the main features of MT: they receive direct V1 input (Kaas *et al*., 1989), are separated from V2 by an additional area and have a large concentration of direction-selective cells. They are, however, relatively lightly myelinated compared with MT. Another difference is the lack of centrifugal anisotropy in areas ML and L, which has been found in MT (Albright, 1989). The similarity between ML/L and MT may be the result of homoplasy or homology. In the first case, the direction selectivity in ML/L is due to parallel evolution, in the second case both ML/L and MT developed from a common ancestor. The presence of a continuous V2 and of direction selectivity in areas ML and L in the squirrel indicate that several elements characterizing the primate visual system are found in rodents. One possibility is that there may be homology between MT, and ML and L. This would imply that, among rodents, rats and other nocturnal rodent species constitute an exceptional case, having differentiated away from the condition shared by the common ancestor of rats, squirrels, primates, cats and other mammals.

According to the alternative hypothesis, the complex organization of squirrel cortex developed *de novo* from a more primitive cortical organization in which V2 and L/ML were absent. This view is probably the most commonly held, given that early mammals appear to have been small nocturnal creatures. Also, the presence of an MT-like area has not been established for most mammalian species. This hypothesis, however, requires that the substantial degree of similarity between squirrels and primates has arisen through parallel evolution.

There is currently not enough information to decide between these two hypotheses. The evolution of motion processing, and consequently the relationship between ML and L and MT, can ultimately be only understood by studying the extrastriate cortex of a larger number of mammals and comparing the results across species.

Notes

This work was supported by NIH grant MH47035 to M.I.S. and by the UCSD McDonnell-Pew Cognitive Neuroscience Center.

Address correspondence to: Monica Paolini, Zoology and Neurobiology ND 7/31, Ruhr University Bochum, D-44787 Bochum, Germany. E-mail: paolini@neurobiologie.ruhr-uni-bochum.de.

References

Albright TD (1984) Direction and orientation selectivity of neurons in area MT of the macaque. J Neurophysiol 52:1106–1130.

Albright TD (1989) Centrifugal bias in the middle temporal visual area (MT) of the macaque. Vis Neurosci 2:177–188.

Allman JM, Miezin F, McGuinness E (1985) Direction- and velocity-specific responses from beyond the classical receptive-fiels in the middle temporal visual area (MT). Perception 14:105–126.

Andersen RA, Snowden RJ, Treue S, Graziano M (1990) Hierarchical processing of motion in the visual cortex of monkey. Cold Spring Harbor Symp Quant Biol 55:741–748.

Baker JF, Petersen SE, Newsome WT, Allman JM (1981) Visual response properties of neurons in four extrastriate visual areas of the owl monkey (*Aotus trivirgatus*): a quantitative comparison of medial, dorsomedial, dorsolateral and middle temporal areas. J Neurophysiol 45:397–416.

Batschelet E (1981) Circular statistics in biology. London: Academic Press.

Bauer R, Dow BM (1989) Complementary global maps for orientation coding in upper and lower layers of the monkey's foveal striate cortex. Exp Brain Res 76:503–509.

Bauer R, Hoffmann KP, Huber HP, Mayr M (1989) Different anisotropies of movement direction in upper and lower layers of the cat's area 18 and their implications for global optic flow processing. Exp Brain Res 74:395–401.

Blakemore C, Zumbroich TJ (1987) Stimulus selectivity and functional organization in the lateral suprasylvian visual cortex of the cat. J Physiol Lond 389:569–603.

Blakeslee B, Jacobs GH, McCourt ME (1985) Anisotropy in the preferred directions and visual field location of directionally-selective optic nerve fibers in the gray squirrel. Vision Res 25:615–618.

Coogan TA, Burkhalter A (1993) Hierarchical organization of areas in rat visual cortex. J Neurosci 13:3749–3772.

Cusick CG, Pons TP, Kaas JH (1980) Some connections of striate cortex (area 17) in the grey squirrel. Soc Neurosci Abstr 10:579.

DeYoe EA, Van Essen DC (1988) Concurrent processing streams in monkey visual cortex. Trends Neurosci 11:219–226.
Felleman DJ, Kaas JH (1984) Receptive field properties of neurons in middle temporal visual area (MT) of owl monkeys. J Neurophysiol 52: 488–513.
Fisher NI (1993) Statistical analysis of circular data. Cambridge: Cambridge University Press.
Gallyas F (1979) Silver staining of myelin by means of physical development. Neurol Res 1:203–209.
Gibson JJ (1950) The perception of the visual world. Boston, MA: Houghton Mifflin.
Gizzi MS, Katz E, Schumer RA, Movshon JA (1990) Selectivity for orientation and direction of motion of single neurons in cat striate and extrastriate visual cortex. J Neurophysiol 63:1529–1543.
Gould HJ (1984) Interhemispheric connections of the visual cortex in the grey squirrel (*Sciurus carolinensis*). J Comp Neurol 223:259–301.
Grant S, Shipp S (1991) Visuotopic organization of the lateral suprasylvian area and of an adjacent area of the ectosylvian gyrus of cat cortex: a physiological and connectional study. Vis Neurosci 6:315–338.
Gur M, Sivak JG (1979) Refractive state of the eye of a small diurnal mammal: the ground squirrel. Am J Optom Physiol Opt 56:689–695.
Hall WC, Kaas JH, Killackey H, Diamond IT (1971) Cortical visual areas in the grey squirrel (*Sciurus carolinesis*): a correlation between cortical evoked potential maps and architectonic subdivisions. J Neurophysiol 34:437–452.
Jones JP, Palmer LA (1987) The two-dimensional spatial structure of simple receptive fields in cat striate cortex. J Neurophysiol 58: 1187–1211.
Kaas JH (1995) The evolution of isocortex. Brain Behav Evol 46:187–196.
Kaas JH, Hall WC, Diamond IT (1972) Visual cortex of the grey squirrel (*Sciurus carolinensis*): architectonic subdivisions and connections from the visual thalamus. J Comp Neurol 145:273–305.
Kaas JH, Krubitzer LA, Johanson KL (1989) Cortical connections of areas 17 (V-I) and 18 (V-II) of squirrels. J Comp Neurol 281:426–446.
Krubitzer LA (1995) The organization of neocortex in mammals: are species really so different? Trends Neurosci 18:408–417.
Livingstone M, Hubel M (1988) Segregation of form, color, movement, and depth: anatomy, physiology and perception. Science 240: 740–749.
Lund JS, Yoshioka T, Levitt JB (1993) Comparison of intrinsic connectivity in different areas of macaque monkey cerebral cortex. Cereb Cortex 3:148–162.
Maunsell JHR, Van Essen DC (1983) Functional properties of neurons in middle temporal visual area of the macaque monkey. 1. Selectivity for stimulus direction, speed and orientation. J Neurophysiol 49: 1127–1147.
Maunsell JHR, Nealey TA, DePriest DD (1990) Magnocellular and parvocellular contributions to responses in the middle temporal visual area (MT) of the macaque monkey. J Neurosci 10:3323–3334.
McCourt ME, Jacobs GH (1984a) Directional filter characteristics of optic nerve fibers in California ground squirrel (*Spermophilus beecheyi*). J Neurophysiol 52:1200–1212.
McCourt ME, Jacobs GH (1984b) Refractive state, depth of focus and accommodation of the eye of the California ground squirrel (*Spermophilus beecheyi*). Vision Res 24:1261–1266.
McLean J, Raab S, Palmer LA (1994) Contribution of linear mechanisms to the specification of local motion by simple cells in areas 17 and 18 of the cat. Vis Neurosci 11:271–294.
Montero VM (1993) Retinotopy of cortical connections between the striate cortex and extrastriate visual areas in the rat. Exp Brain Res 94:1–15.
Montero VM, Cliffer KD (1981) Cortical connections from the striate cortex in the gray squirrel: definition of extrastriate cortical visual areas. Soc Neurosci Abstr 11:763.
Montero VM, Rojas A, Torrealba F (1973) Retinotopic organization of striate and peristriate visual cortex in the albino rat. Brain Res 53:197–201.
Neitz J, Jacobs GH (1986) Reexamination of spectral mechanisms in the rat (*Rattus norvegicus*). J Comp Psychol 100:21–29.
Northcutt RG, Kaas JH (1995) The emergence and evolution of mammalian neocortex. Trends Neurosci 18:373–379.
Olavarria J, Mendez B (1979) The representations of the visual field on the posterior cortex of *Octodon degus*. Brain Res 161:539–543.
Olavarria J, Montero VM (1984) Relation of callosal and striate–extrastriate cortical connections in the rat: morphological definition of extrastriate visual areas. Exp Brain Res 54:240–252.
Olavarria J, Van Sluyters RC (1985) Unfolding and flattening the cortex of gyrencephalic brains. J Neurosci 15:191–202.
Palmer LA, Jones JP, Stepnoski A (1991) Striate receptive fields: characterization in two dimensions of space. In: The neural basis of visual attention (Leventhal A, ed.), pp. 246–265. Boca Raton, FL: The Macmillan Press.
Paolini M, Freeling N, Sereno MI (1995) Motion processing in extrastriate cortical areas in the California ground squirrel. Soc Neurosci Abstr 25:280.
Payne BR (1993) Evidence for visual cortical area homologs in cat and macaque monkey. Cereb Cortex 3:1–25.
Rauschecker JP, von Grunau MW, Poulin C (1987) Centrifugal organization of direction preferences in cat's lateral suprasylvian visual cortex and its relation to flow field processing. J Neurosci 7:943–958.
Revishchin AV, Polkoshnikov EV (1987) [Topical organization of visual cortico-cortical connections in the squirrel. Double retrograde tracing.] Topicheskaia organizatsiia zritel'nykh kortiko-kortikal'nykh sviazei u belki. Dvoinoe retrogradnoe proslezhivanie. Dokl Akad Nauk SSSR 294:226–229.
Ringach DL, Hawken MJ, Shapley R (1997) Dynamics of orientation tuning in macaque primary visual cortex. Nature 387:281–284.
Sereno MI, Rodman HR, Karten HJ (1991) Organization of visual cortex in the California ground squirrel. Soc Neurosci Abstr 17:844.
Sherk H, Kim JN, Mulligan K (1995) Are the preferred directions of neurons in cat extrastriate cortex related to optic flow? Vis Neurosci 12:887–894.
Spear PD, Baumann TP (1975) Receptive-field characteristics of single neurons in lateral suprasylvian visual area of the cat. J Neurophysiol 38:1403–1420.
Tootell RBH, Silverman MS (1985) Two methods for flat-mounting cortical tissue. J Neurosci Methods 15:177–190.
Toyama K, Mizobe K, Akase E, Kaihara T (1994) Neuronal responsiveness in areas 19 and 21a, and the posteromedial lateral suprasylvian cortex of the cat. Exp Brain Res 99:289–301.
Van Essen DC, Anderson CH, Felleman DJ (1992) Information processing in ther primate visual system: an integrated systems perspective. Science 255:419–428.
Vogels R, Orban GA (1990) How well do response changes of striate neurons signal differences in orientation: a study in the discriminating monkey. J Neurosci 10:3543–3558.
von Grunau M, Frost B (1983) Double-opponent-process mechanism underlying RF-structure of directionally specific cells of cat lateral suprasylvian visual area. Exp Brain Res 49:84–92.
Wang Y, Frost BJ (1992) Time to collision is signaled by neurons in the locus rotundus of pigeon. Nature 356:236–238.
Wang Y, Wang L, Li B, Wang LM, Diao YC (1995) How is direction selectivity organized in the extrastriate visual area PMLS of the cat? Neuroreport 6:1969–1974.
Wurtz RH, Yamasaki DS, Duffy CJ, Roy JP (1990) Functional specialization for visual motion processing in primate cerebral cortex. Cold Spring Harbor Symp Quant Biol 55:717–727.
Young MP (1992) Objective analysis of the topological organization of the primate cortical visual system. Nature 358:152–155.
Zar JH (1996) Biostatistical analysis. Upper Saddle River, NJ: Prentice Hall.
Zeki SM (1974) Functional organization of a visual area in the posterior bank of the superior temporal sulcus of the rhesus monkey. J Physiol Lond 236:549–573.